Hindawi Publishing Corporation
Mathematical Problems in Engineering
Volume 2013, Article ID 875376, 8 pages
http://dx.doi.org/10.1155/2013/875376

Research Article

FEM Analysis of Dynamic Response of Buried Fiber Reinforced Plastic Matrix Pipe under Seismic Load

Xu Lei,[1] Ye Zhicai,[2] Ren Qingwen,[3] and Zhang Lei[4]

[1] *College of Water Conservancy and Hydropower Engineering, Hohai University, Nanjing 210098, China*
[2] *Suqian Water Authority, Suqian 223800, China*
[3] *College of Mechanics and Materials, Hohai University, Nanjing 210098, China*
[4] *China Institute of Water Resources and Hydropower Research, Beijing 100038, China*

Correspondence should be addressed to Xu Lei; leixu@hhu.edu.cn

Received 18 July 2013; Accepted 15 September 2013

Academic Editor: Zhiqiang Hu

Fiber reinforced plastic matrix pipes have been widely used in the field of civil engineering and hydraulic engineering. In general, the existing FEM models used in the seismic analysis of buried pipes do not fully consider the dynamic interaction between pipe and surrounding soil, and most of the models are proposed for homogeneous pipe. Therefore, the existing models cannot be directly applied to the seismic analysis of fiber reinforced plastic matrix pipes with laminated structure. Based on the aforementioned, the FEM model for the seismic analysis of fiber reinforced plastic matrix pipes is presented by taking consideration of the laminated structure, the complicated dynamic interaction between pipe and surrounding soil, and the propagation of seismic scattering waves from finite field to infinite field. The analysis results of a project case show that the proposed model can reasonably analyse the dynamic response of buried fiber reinforced plastic matrix pipes under seismic load.

1. Introduction

With the sustained and rapid infrastructure construction to be carried out in China, the fiber reinforced plastic matrix pipe (hereafter be shorted as FRPM pipe) with the advantages of light weight, high stiffness, good water delivery performance, and convenient construction has been widely used in the field of civil engineering and hydraulic engineering [1–3]. Generally, the FRPM pipes are buried under the ground, and buried pipes often suffer serious damage during the seismic motion [4]. China is an earthquake-prone country, whose region with the basic seismic intensity above 6 degree is accounted for more than 60% of the country's total area. Thus, it is important to make a reasonable dynamic response analysis of buried pipes under seismic load and improve their seismic safety.

Recently, some FEM models for seismic analysis of buried homogeneous pipe have been established [5–8]. Most of them do not fully consider the dynamic interaction between pipe and surrounding soil, and the study on the homogeneous pipe in the literature [7] has taken consideration of the interaction of soil and pipe using ADINA. On the other hand, as the FRPM pipe is a layered composite pipe [2, 3], which shows different deformation and stress features from homogeneous pipe, it is necessary to establish a FEM model for seismic analysis of buried FRPM pipe.

In view of this, the FEM model for seismic analysis of buried FRPM pipe is presented by taking consideration of the composite laminated structure characteristic, the complicated dynamic interaction between pipe and surrounding soil, and the propagation of seismic scattering waves from finite field to infinite field. The analysis results of a project case show that the proposed model can reasonably analyse the dynamic response of buried FRPM pipe under seismic load.

2. Establishment of the Seismic Analysis Model

2.1. The FEM Model Based on Laminated Shell Element. Generally, the ratio of FRPM pipe thickness relative to its diameter is less than 1/15, so it is suitable to simulate the FRPM pipe using shell element. In addition, the FRPM

pipe is a typically laminated structure, so it is necessary to consider this feature in the FEM model. Therefore, the shell element should be divided into several layers of different materials along the thickness direction, and all layers of the shell element should be analyzed as a whole element in the calculation process. For convenient, the laminated shell element in ABAQUS which can meet the above requirement is chosen.

The laminated shell element can be divided into several material layers of different thickness along the shell thickness direction, but the number of nodes, basic unknown quantity, and the rank of the element stiffness matrix are still the same as traditional shell element. The element stiffness matrix and the element equivalent nodal force are calculated through numerical integration based on the cross-sectional properties of the given laminated shell element which are the thickness, the number of integration points, and the constitutive model of each layer.

In general, FRPM pipe can be divided into the outer surface layer, the inner liner layer, and the structure layer. The outer surface layer, the inner liner layer, and the sand inclusion layer of the structure layer can be viewed as an isotropic elastic material, while the glass fiber layer with different winding way should be regarded as an orthotropic elastic material.

2.2. Contact Simulation of Dynamic Interaction between Pipe and Soil. Essentially, the interaction between pipe and surrounding soil is a contact problem. Thus, the contact analysis function of ABAQUS is used to simulate the dynamic interaction between pipe and soil in the seismic analysis model for buried FRPM pipe.

Since the FRPM pipe is harder than surrounding soil, the FRPM pipe surface that contacts the soil is set as the master contact surface, and the soil surface that contacts the FRPM pipe surface is set as the slave contact surface. In order to achieve a satisfied result, the mesh density of the soil surface should not be less than that of FRPM pipe surface. Based on the interaction mechanism between the FRPM pipe and the surrounding soil, the classical isotropic coulomb friction model is used to describe the tangential contact property between pipe and soil, and the hard contact model is adopted, which allows normal separation and does not allow normal aggression, to describe the normal contact property between pipe and soil.

2.3. Viscoelastic Artificial Dynamic Boundary Condition. For the seismic analysis of buried FRPM pipe, a limited scope is artificially intercepted to simulate an infinite foundation. Thus, how to eliminate the reflection of seismic wave on the truncated boundary is a key problem which affects the rationality of the analysis results of seismic response, and how to set a reasonable dynamic artificial boundary condition in the intercepted finite field boundary is an effective method to solve this problem. Among several artificial boundaries, the viscoelastic artificial boundary with high precision and frequency stability is widely used in FEM analysis of the structure-foundation dynamic interaction for its good performance to simulate the elastic recovery of the semi-infinite medium outside the artificial boundary.

The viscoelastic dynamic artificial boundary is equivalent to continuous distributional parallel spring-damper system which is distributed in the truncation boundary of the computational model. The spring coefficient K_b and damping coefficient C_b is calculated as follows:

$$K_b = \alpha \frac{G}{R}, \qquad C_b = \rho c, \tag{1}$$

where G, ρ are shear modulus and density, respectively; R is the distance from scattering wave source to the artificial boundary; c is the wave velocity at artificial boundary, which takes the value of longitudinal wave velocity c_p when calculating the normal damping coefficient and takes the value of shear wave velocity c_s when calculating tangential damping coefficient; the value of α depends on the type and direction of the viscoelastic artificial boundary.

For the FEM analysis of the structure-foundation dynamic interaction in practical engineering, the distance from each boundary node to scattering wave source is not equal. The boundary area controlled by node is different, and the represented materials of nodes are also different. Thus, it is a very tedious work to calculate the spring coefficient and damping coefficient and add spring element and damper element for each boundary node. To solve this problem, a new method [9] is proposed based on the viscoelastic dynamic artificial boundary theory, by which the viscoelastic artificial boundary is accurately and automatically applied, and the corresponding program module is developed based on ABAQUS. The process of exerting the viscoelastic boundary in ABAQUS is simply divided into two steps. First step, the spring and damping coefficient of the node on the boundary should be calculated considering the foundation mechanical parameters and the area represented by the node. Second step, the spring element SPRING1 and damping element DASHPOT1 is used to exert the spring and the viscous damping, and two types of element mentioned above have a common node with the FEM model, and the other node is considered as fixed at foundation.

The viscoelastic artificial boundary is applied to simulate the seismic scattering wave propagation from finite field to infinite field in the proposed seismic analysis model for buried FRPM pipe, and its realization method is given in detail in the literature [9].

2.4. Synthesis of Artificial Seismic Wave and Seismic Motion Input. In order to make a reasonable dynamic response analysis of the buried FRPM pipe under seismic load, artificial seismic wave should comply with the requirement of the specific project site condition. Generally, the existing measured seismic wave is difficult to meet the requirement, so the artificial seismic wave should be synthesized.

Recently, the theory of artificial earthquake synthesis develops rapidly, and the related scholars develop many FORTRAN programs used to synthesize the artificial seismic waves. But most of these programs are nonvisual, inconvenient to use, have low efficiency, and poor portability. In

view of this, the visual software SCAEW for the synthesis of artificial seismic wave is developed based on the GUI development environment of MATLAB software platform and the theory of artificial earthquake synthesis [10].

In the development of the software, the seismic acceleration wave is considered as a nonstationary random process as shown in (2), which is the product of a stationary random process and an envelope function. The theory of artificial earthquake synthesis used in the software is described in detail in the literature [10]:

$$a(t) = f(t)\, a_s(t), \tag{2}$$

where $a(t)$ is the seismic acceleration time history; $f(t)$ is the envelope function; $a_s(t)$ is a Gauss stationary random process with zero mean and unilateral power spectral density function.

In the process of FEM analysis of the buried FRPM pipe, the artificial seismic wave is synthesized using SCAEW.

On the other hand, seismic motion should be reasonably applied to the computational model when viscoelastic boundary is used in the seismic analysis of the buried FRPM pipe. Based on the principle of separation of the wave field, the wave field on the artificial boundary can be divided into the free seismic wave field and the scattered wave field. The scattering wave propagation to the infinite domain will automatically be satisfied by using the viscoelastic boundary, and only the free seismic wave field should be applied to the boundary. The input of the free seismic wave field can be realized through applying the equivalent load to the artificial boundary nodes, and the equivalent load can be calculated as follows [11]:

$$F_b = \tau + C_b \dot{u} + K_b u, \tag{3}$$

where F_b is the equivalent load at artificial boundary; τ is the dynamic stress of the free seismic wave field generated at the artificial boundary; $u, \dot{u}$ are the displacement and speed of the seismic wave field, respectively.

3. Project Case Analysis

Based on the aforementioned, the establishment of seismic analysis FEM model of the buried FRPM pipe is completed. The following project case analysis illustrates the validity and reasonableness of the proposed model.

3.1. Project Overview and Computational Parameters. A FRPM pipe, diameter 600 mm, stiffness level 10000 Pa, and wall thickness 13.2 mm, is used as water pipe in eastern route of the south-to-north water diversion project which is shown in Figure 1. The designed layers are as follows: the inside liner thickness is 2 mm; the thickness of toroidal winding layer of glass fiber is 1.236 mm; the thickness of cross winding layer of glass fiber is 0.996 mm; the thickness of toroidal winding layer of glass fiber is 0.824 mm; the thickness of clip sand layer is 4.5 mm; the thickness of toroidal winding layer of glass fiber is 0.824 mm; the thickness of cross winding layer of glass fiber is 1.992 mm; the thickness of toroidal winding layer of glass fiber is 0.828 mm; the winding angle of cross winding layer of glass fiber is 57.52°.

Figure 1: Project layout.

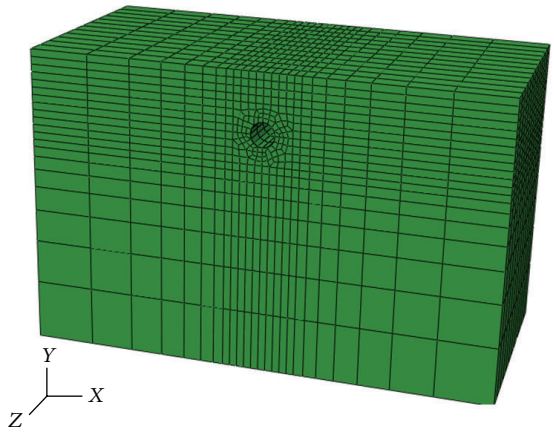

Figure 2: Global FEM model.

In the process of FEM model establishment, the inside liner layer and the RPM layer are considered as isotropic material, and the wound layer is regarded as an orthotropic

Table 1: The physical and mechanical parameters of soil layers.

Soil layers	Elastic modulus (MPa)	Poisson's ratio	Cohesive force (kPa)	Internal friction angle (°)	Proportion
Backfill	25.00	0.3	20.80	12.00	1.80
Sandy loam soil	29.45	0.3	26.00	15.00	2.71
Floury soil	66.80	0.3	7.00	21.00	2.70
Clay	44.40	0.3	56.00	17.00	2.80

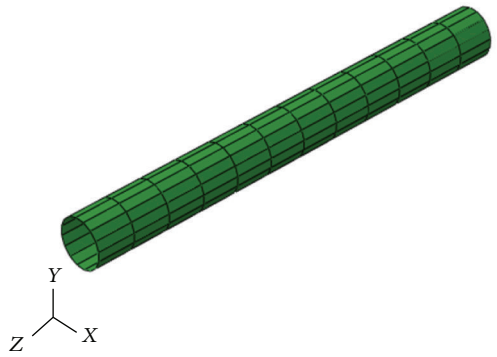

Figure 3: FEM mesh of FRPM pipe.

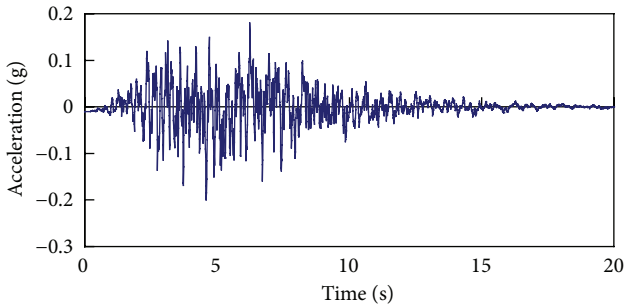

Figure 4: Acceleration time series.

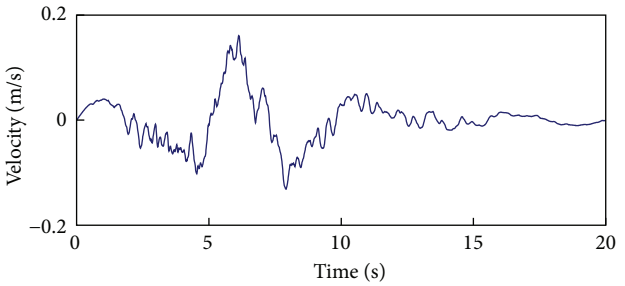

Figure 5: Velocity time series.

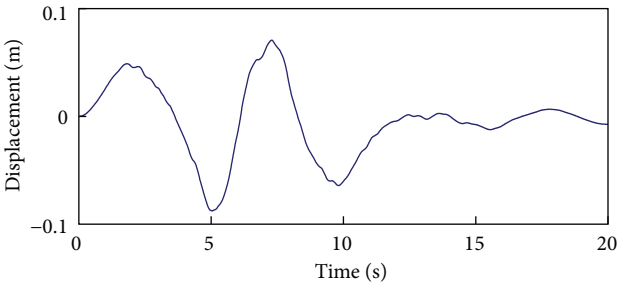

Figure 6: Displacement time series.

material. The material parameters of different layers are as follows.

Inside Liner. Elasticity modulus is 6.74 GPa; the Poisson's ratio is 0.33.

Toroidal Winding Layer. longitudinal elasticity modulus is 38 GPa; transverse elasticity modulus is 6.9 GPa; Poisson's ratio is 0.27; shear elasticity modulus is 3.8 GPa.

Cross Winding Layer. Longitudinal elasticity modulus is 70 GPa; transverse elasticity modulus is 7.6 GPa; Poisson's ratio is 0.3; shear elasticity modulus is 4.79 GPa.

Clip Sand Layer. Elasticity modulus is 6.4 GPa; Poisson's ratio is 0.33.

The physical and mechanical parameters of the surrounding soil are shown in Table 1. The dynamic friction parameter between pipe and soil is taken as 0.15.

According to the Chinese Earthquake Motion Parameter Zoning Map (GB18306-2001), the basic seismic intensity in the engineering area is 8 degree, and the characteristic period of earthquake motion response spectrum is 0.35 s.

3.2. FEM Model and Boundary Conditions. The water pipe, which is covered by 1.2 m thick soil, has a length of 6 m, and the diameter of pipe is 0.6 m. The laminated shell element is used to simulate the pipe, and the pipe is homogeneously meshed by 12 elements in the pipeline axial direction and 16 elements in the pipeline toroidal direction. The laminated shell element is divided into 8 layers in the thickness direction according to the design of the pipe layer. The left boundary, the right boundary, and the bottom boundary of FEM model are set at 10 times of the nominal pipe diameter away from the center of pipe cross-section, and the up surface is the ground surface. The FEM mesh has 6348 elements and 7553 nodes. The FRPM pipe is meshed by 192 laminated shell elements, and the soil is meshed by 6156 8-node hexahedral elements. The global FEM model and the FEM model of FRMP pipe are shown in Figures 2 and 3.

The viscoelastic boundary is accurately and automatically applied to the FEM model by using the method proposed in the literature [9]. The spring coefficient K_b is taken as 2.0 in tangential direction and 4.0 in normal direction.

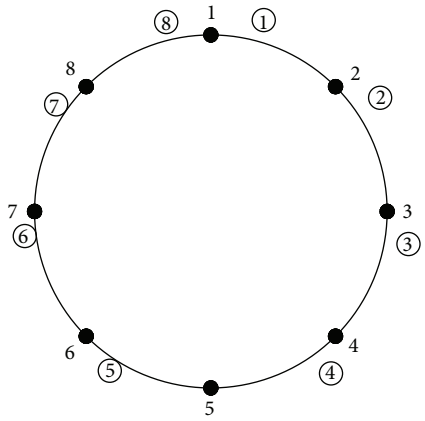

Figure 7: Sketch of key points and key elements position.

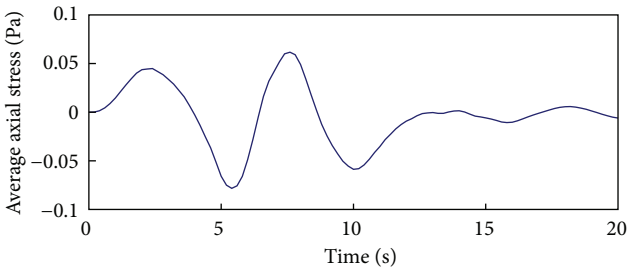

Figure 8: The x direction displacement time series of key point 1.

3.3. Artificial Seismic Wave Synthesis. By using trigonometric series method and taking the standard response spectrum of Code for Seismic Design of Hydraulic Structures as the target spectrum, the time histories of seismic acceleration, seismic velocity, and seismic displacement are synthesized using the software SCAEW. The time history curves of seismic acceleration, seismic velocity, and seismic displacement are given in Figures 4, 5, and 6. The coupling interaction between horizontal seismic excitation and vertical seismic excitation in calculation is considered, and the value of vertical seismic peak acceleration is taken as 2/3 of the value of the horizontal seismic peak acceleration according to the seismic design specification.

3.4. Analysis of Calculation Results. Dynamic time-history FEM analysis is accomplished by using of ABAQUS, and the step time is taken as 0.02 s. In order to understand the deformation and impulse load of the pipe under seismic load, the nodes and the laminated shell elements in the mid-part of the pipe are chosen to study. For convenient expression, the key nodes and the key elements indicated by the digital serial number represent the different parts of the pipe, as shown in Figure 7.

As the size of the pipe is small, the displacement-time curves of the all key nodes are almost the same, and Figure 8 shows the displacement-time curve in the x direction (horizontal transverse direction) of the key node 1 in the mid-part of the pipe section. The displacement of pipe varying

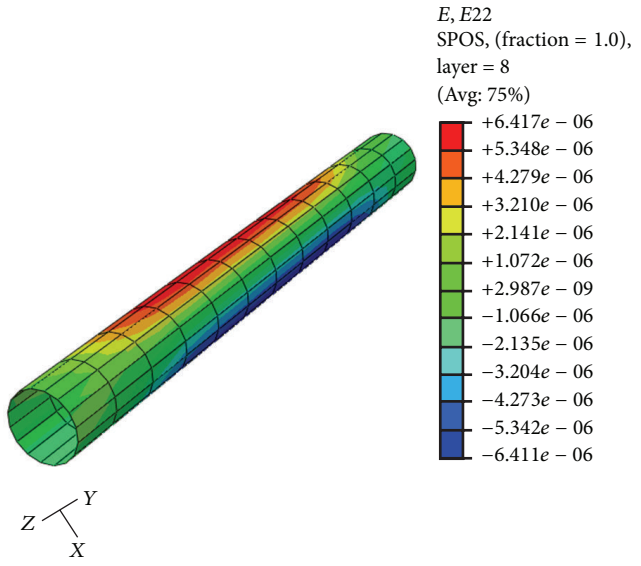

Figure 9: The pipe contour of axial strain (t = 5.4 s).

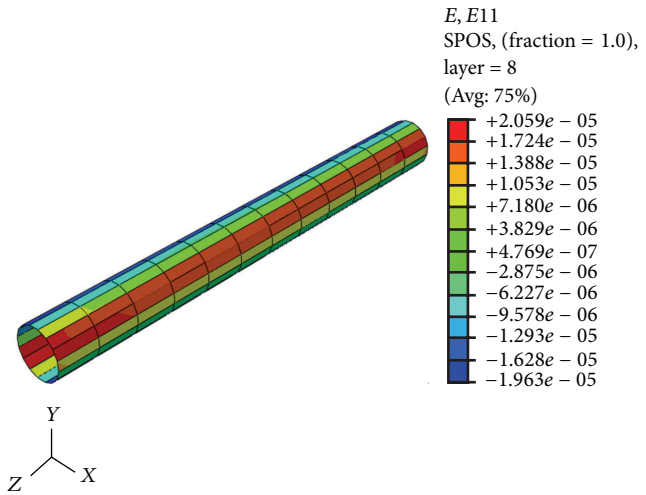

Figure 10: The pipe contour of hoop strain (t = 5.4 s).

with time is basically identical with seismic motion, which reflects the restraining action of the soil around pipe and the deformation of the pipe mainly depends on the imposition of the surrounding soil. The maximum displacement in the x direction of the mid-part of the pipe occurs in the lower-right part of the pipe wall (z-axis negative perspective), and its occurring time and magnitude are 5.4 s and −0.079 m, respectively. The contour of the axial strain and hoop strain of the pipe wall surface are shown in Figures 9 and 10. From Figure 9 it can be seen that the maximum of the pipe axial strain is located in the mid-part of the pipe. The obvious antisymmetric distribution characteristics are presented in the both sides of the pipe wall, and the left side is in tension (positive), while the right side is in compression (negative). The value is small, and the maximum value is 6.417$\mu\varepsilon$ at this moment. From Figure 10, it can be seen that the hoop strain

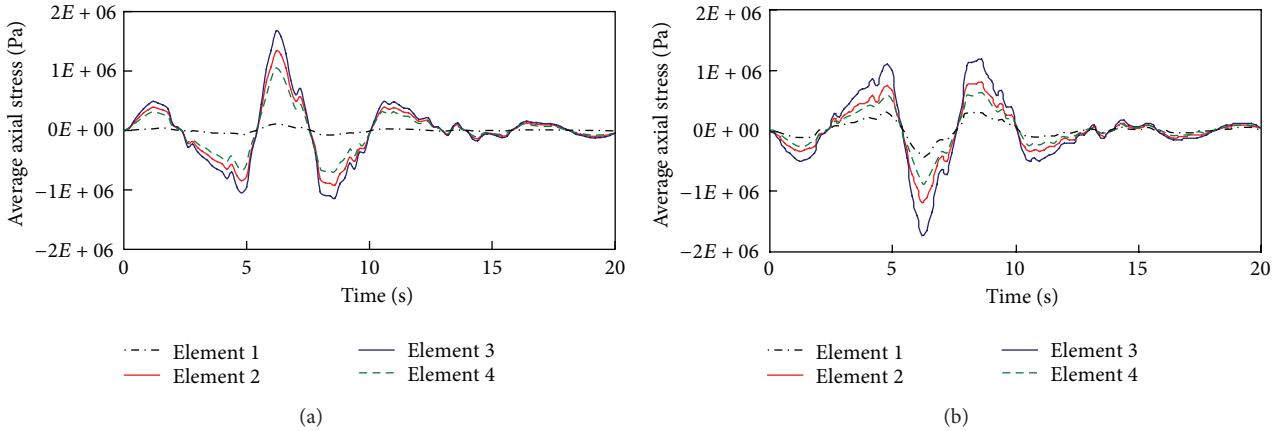

Figure 11: Time series of average axial stress.

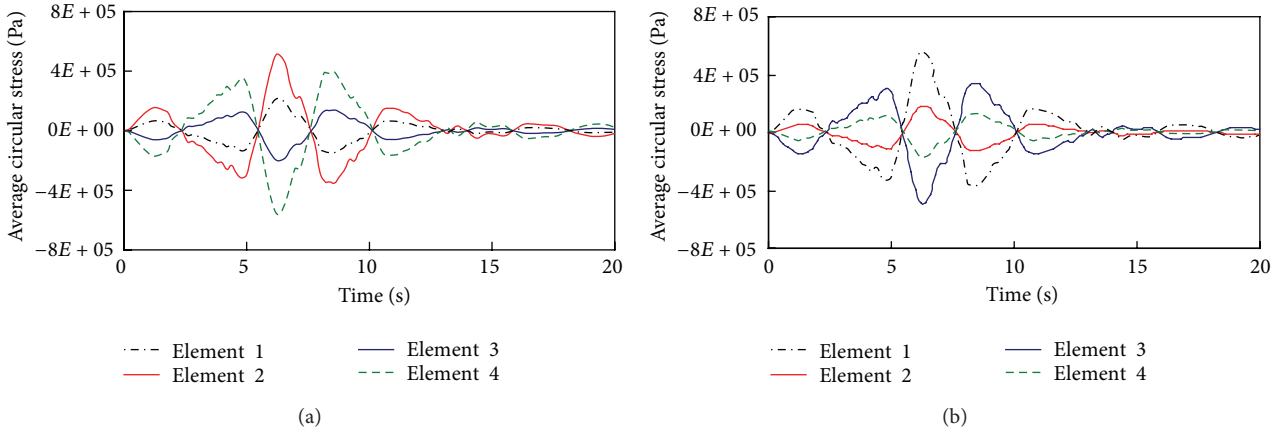

Figure 12: Time series of average circular stress.

distribution of the pipe wall is symmetric in axial direction (vertical). The region of the tensile in the hoop direction is located at the lower-left and the lower-right parts of the pipe wall, while the region of the compression is located at the upper-left and the upper-right part of the pipe wall. The maximum hoop strain is 20.059$\mu\varepsilon$ at this moment.

The average axial stress time history curve and the average hoop stress time history curve of each key element in the middle part of the pipe section are shown in Figures 11 and 12, and the average axial stress and the average hoop stress are the weighed average stress, which is calculated based on the weight of the thickness of each layer according to the ply design of FRPM pipe.

From Figure 11, it can be seen that the average axial stress time history is approximately antisymmetric to y-axis (vertical transverse), and the stress value of the pipe waist position is bigger than the stress value of the position of the top and bottom. From Figure 12, it can be seen that the average hoop stress of the pipe wall on the left and right is antisymmetric x-axis. The tensile region is located at the upper-left part of the pipe wall, while the compression region

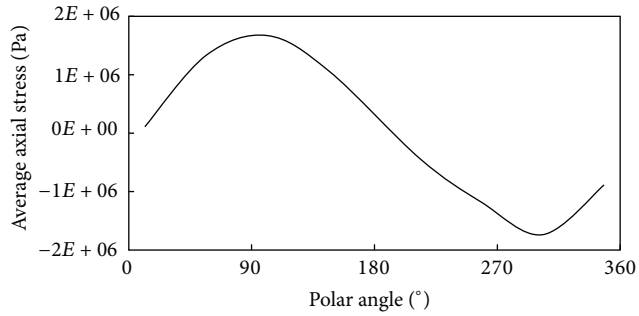

Figure 13: The average axial stress along pipe wall.

is located at the lower-left part of the pipe wall. In general, it can be considered that the distribution of the average hoop stress of the pipe wall is centrosymmetric to the pipe axis. In addition, the average hoop stress of the pipe wall is less than the average axial stress.

From Figures 13 and 14, it can be seen that the average axial stress and the average hoop stress of each element in

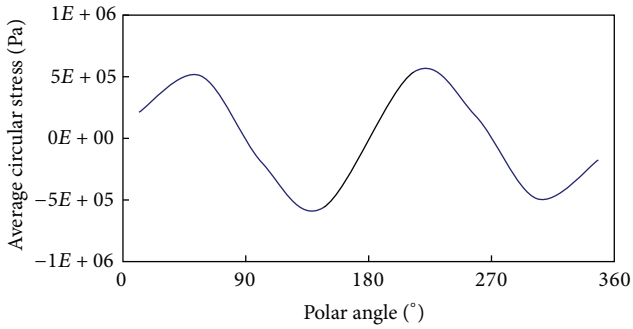

Figure 14: The average circular stress along pipe wall.

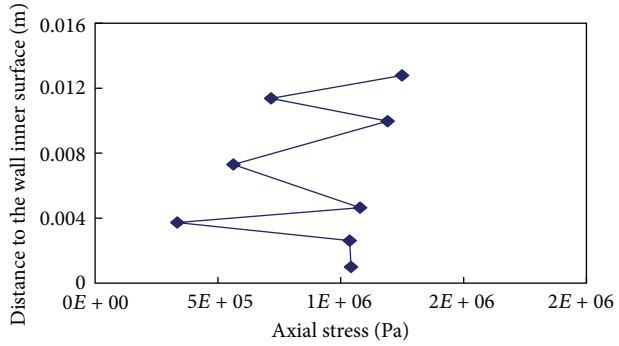

Figure 15: The axial stress along thickness direction (t = 6.2 s, element ③).

the mid-part of the pipe wall change through polar angle (a predetermined angle in a clockwise direction; the polar angle of the top of the buried pipe is taken as 0°).

From Figure 13, it can be seen that from the top of the pipe to the bottom of the pipe along the right part of the pipe, the value of average axial tension stress changes from small to large and then changes to small; from the bottom of the pipe wall to the bottom of the pipe along the left part of the pipe, the value of average axial compression stress changes from small to large and then changes to small. The maximum value is located at the pipe waist.

From Figure 14, it can be seen that the average hoop stress of the upper part and the lower part in both sides is antisymmetric. As a whole, the average hoop stress is symmetric to the pipe wall center, and the tensile region is located at the upper-right part and upper-left part of the pipe wall, while the compression region is located at the lower-left part and lower-right part of the pipe wall.

The average stress of FRPM pipe wall is analyzed above, but in fact the FRPM pipe is a layered composites pipe. The FRPM pipe is divided into 8 layers and the material property of each layer is different. The axial stress and hoop stress of each layer at the time when the peak value of average axial stress is achieved are shown in Figures 15 and 16. The axial stress and hoop stress of each layer in FRPM pipe are different from cross-sectional average stress, and the stress of each layer is different. For axial stress, the stress sign of each layer is the same and the value of each layer stress is related to the elastic modulus of each layer. The bigger the elastic modulus is, the bigger the stress is. In addition, the axial stress is linearly increased from the internal surface to outer surface of pipe wall for the layers which have similar elastic modulus.

As the result of the deformation of the surrounding soil, the deformation of the pipe is complicated and the bending deformation exists. The hoop stress sign is not the same and depends on the relative position of the layer to the neutral surface of the pipe wall. In addition, with the similarity to the axial stress, the value of the hoop stress is decided by the value of elastic modulus of each layer.

Based on the aforementioned, it can be concluded that the proposed model can give a reasonable and effective seismic analysis of the buried FRPM pipe.

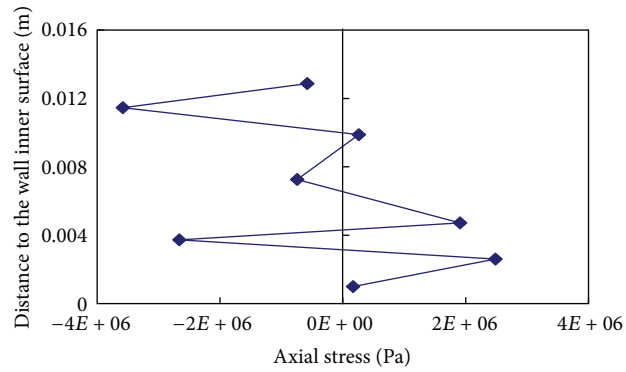

Figure 16: The hoop stress along thickness direction (t = 6.2 s, element ⑥).

4. Conclusions

FRPM pipes have been widely used in the field of civil engineering and hydraulic engineering, but the appropriate FEM model for seismic analysis of buried FRPM pipes does not exist. In view of this, the seismic FEM model for buried FRPM pipes is presented based on the laminated shell element in ABAQUS by taking consideration of the complicated interaction of pipe and surrounding soil and the propagation of seismic scattering waves from finite field to infinite field using viscoelastic dynamic boundary. The results of a project show that the proposed model can reasonably analyse the dynamic response of buried FRPM pipe under seismic load.

Conflict of Interests

The authors do not have any conflict of interests with the content of the paper.

Acknowledgment

This work was supported by projects of the National Natural Science Foundation of China (Grant nos. 51109067, 11132003, and 51079045).

References

[1] L. Yong, W. Fan, and L. Renhuai, "Bending analysis of FRMP pipes of filament-wound under external loads," *Journal of Jinan University*, vol. 26, no. 1, pp. 16–19, 2005.

[2] L. Yan, "Application of FRP/GRP pipe in Pingshang emergency water diversion project," *China Water Resources*, no. 4, pp. 23–25, 2009.

[3] S. Jihong, W. Huiming, S. Xiaolei et al., "Glass fiber reinforced mortar pipe optimization design based on finite element analysis," *Journal of Shihezi University*, vol. 26, no. 2, pp. 228–231, 2008.

[4] L. Hongnan, X. Shiyun, and H. Linsheng, "Damage investigation and analysis of engineering structures in the Wenchuan earthquake," *Chinese Journal of Building Structures*, vol. 29, no. 4, pp. 10–19, 2008.

[5] T. K. Datta, "Seismic response of buried pipelines: a state-of-the-art review," *Nuclear Engineering and Design*, vol. 192, no. 2, pp. 271–284, 1999.

[6] S. W. Liu, S. K. Datta, K. R. Khair, and A. H. Shah, "Three dimensional dynamics of pipelines buried in backfilled trenches due to oblique incidence of body waves," *Soil Dynamics and Earthquake Engineering*, vol. 10, no. 4, pp. 182–191, 2003.

[7] W. Shaojie, Z. Qinjie, L. Yingli et al., "Research on earthquake resistance of buried pipeline under pipe-soil interaction," *Chinese Journal of World Earthquake Engineering*, vol. 23, no. 1, pp. 47–50, 2007.

[8] Z. Xiaoling, L. Maotian, G. Ying et al., "Numerical analysis of dynamic response of saturated porous seabed-pipeline under seismic loading," *Chinese Journal of Rock Mechanics and Engineering*, vol. 27, no. 2, pp. 3798–3806, 2008.

[9] X. Lei, Y. Zhicai, R. Qingwen et al., "The accurate auto-application of viscous-spring dynamic artificial boundary based on ABAQUS," *Journal of China Three Gorges University*, vol. 32, no. 1, pp. 20–23, 2010.

[10] X. Lei, Y. Zhicai, and R. Qingwen, "Development of artificial seismic wave generation visual soft based on MATLAB," *Chinese Journal of Water Resources and Power*, vol. 28, no. 11, pp. 120–122, 2010.

[11] L. Jingbo, D. Yixin, and Y. Qiushi, "The implementation of viscous-spring dynamic artificial boundary and earthquake input in general FEM software," *Chinese Journal of Disaster Prevention and Mitigation Engineering*, vol. 27, no. 1, pp. 37–42, 2007.